Title

Expansion of Gamma-Butyrolactone Signaling Molecule Biosynthesis to Phosphotriester Natural Products

Journal

ACS Chemical Biology, 15(12)

ISSN

1554-8929

Authors

Kudo, Yuta
Awakawa, Takayoshi
Du, Yi-Ling
et al.

Publication Date

2020-12-18

DOI

10.1021/acschembio.0c00824

Peer reviewed

HHS Public Access

Author manuscript

ACS Chem Biol. Author manuscript; available in PMC 2021 December 18.

Published in final edited form as:

ACS Chem Biol. 2020 December 18; 15(12): 3253–3261. doi:10.1021/acschembio.0c00824.

Expansion of Gamma-Butyrolactone Signaling Molecule Biosynthesis to Phosphotriester Natural Products

Yuta Kudo,
Center for Marine Biotechnology and Biomedicine, Scripps Institution of Oceanography, University of California San Diego, La Jolla, California 92093, United States; Frontier Research Institute for Interdisciplinary Sciences and Graduate School of Agricultural Science, Tohoku University, Sendai, Miyagi 980-8578, Japan

Takayoshi Awakawa,
Center for Marine Biotechnology and Biomedicine, Scripps Institution of Oceanography, University of California San Diego, La Jolla, California 92093, United States; Graduate School of Pharmaceutical Sciences, The University of Tokyo, Tokyo 113-0033, Japan

Yi-Ling Du,
Department of Chemistry, University of British Columbia, Vancouver, British Columbia V6T 1Z1, Canada

Peter A. Jordan,
Center for Marine Biotechnology and Biomedicine, Scripps Institution of Oceanography, University of California San Diego, La Jolla, California 92093, United States

Kaitlin E. Creamer,
Center for Marine Biotechnology and Biomedicine, Scripps Institution of Oceanography, University of California San Diego, La Jolla, California 92093, United States

Paul R. Jensen,
Center for Marine Biotechnology and Biomedicine, Scripps Institution of Oceanography, University of California San Diego, La Jolla, California 92093, United States

Roger G. Linington,
Department of Chemistry, Simon Fraser University, Burnaby, British Columbia V5A 1S6, Canada

Katherine S. Ryan,
Department of Chemistry, University of British Columbia, Vancouver, British Columbia V6T 1Z1, Canada

Corresponding Author Bradley S. Moore – Center for Marine Biotechnology and Biomedicine, Scripps Institution of Oceanography and Skaggs School of Pharmacy and Pharmaceutical Sciences, University of California San Diego, La Jolla, California 92093, United States; Phone: 858-822-6650; bsmoore@ucsd.edu.

ASSOCIATED CONTENT

Supporting Information

The Supporting Information is available free of charge at https://pubs.acs.org/doi/10.1021/acschembio.0c00824.
Supplemental methods for general methods, bacterial strains, expression and purification of proteins, dephosphorylation of 8, extraction and purification of 2 and salinipostins, and chemical synthesis of 3–5 and 8; NMR table of 2; HRMS spectra for 2 and 3; MS/MS spectra of 7, 9, and salinipostins; LC-MS chromatograms of 3, 8, 9, and salinipostins; SDS-PAGE of Spt9 and Spt6; NMR spectra for 2–5, 8; CD spectrum for 2 (PDF)

The authors declare no competing financial interest.

Bradley S. Moore
Center for Marine Biotechnology and Biomedicine, Scripps Institution of Oceanography and Skaggs School of Pharmacy and Pharmaceutical Sciences, University of California San Diego, La Jolla, California 92093, United States

Abstract

Bacterial hormones, such as the iconic gamma-butyrolactone A-factor, are essential signaling molecules that regulate diverse physiological processes, including specialized metabolism. These low molecular weight compounds are common in *Streptomyces* species and display species–specific structural differences. Recently, unusual gamma-butyrolactone natural products called salinipostins were isolated from the marine actinomycete genus *Salinispora* based on their antimalarial properties. As the salinipostins possess a rare phosphotriester motif of unknown biosynthetic origin, we set out to explore its construction by the widely conserved 9-gene *spt* operon in *Salinispora* species. We show through a series of *in vivo* and *in vitro* studies that the *spt* gene cluster dually encodes the salinipostins and newly identified natural A-factor-like gamma-butyrolactones (Sal-GBLs). Remarkably, homologous biosynthetic gene clusters are widely distributed among many actinomycete genera, including *Streptomyces*, suggesting the significance of this operon in bacteria.

Graphical Abstract

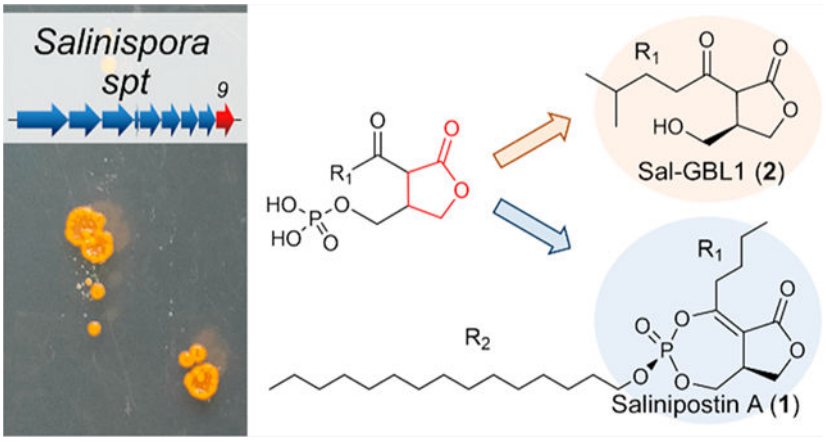

INTRODUCTION

Actinobacteria are a rich source of specialized metabolites that have been developed into life-saving drugs. Recent advances in genome sequencing and mining have revealed that Actinobacteria have far greater potential for secondary metabolite production than previously realized.[1] Yet, much of this potential remains cryptic, as many biosynthetic genes are poorly expressed in normal laboratory incubation conditions.[2] The manipulation of the signaling mechanisms for gene expression can be a key to activating the expression of dormant biosynthetic genes.[3–5] However, the regulation of biosynthetic pathways, and the autoregulators themselves, remains poorly understood.

Among the known signaling molecules, gamma-butyrolactones (GBLs) are recognized to be involved in the regulation of morphological development and secondary metabolism in actinomycete bacteria, especially in the genus of *Streptomyces*.[6–10] In contrast, among the metabolically prolific marine actinomycete genus *Salinispora*, far less is known about the signaling pathways regulating the biosynthesis of their rich repertoire of natural products.[11–15] However, the recently reported potent and selective antimalarial compounds, salinipostins (Figure 1A, salinipostin A (1)) from *Salinispora* sp. RL08-036-SPS-B,[16,17] may shed some light on this. Salinipostins possess a GBL ring analogous to A-factor, as well as a highly unusual phosphotriester ring. Two compounds, cyclipostins and cyclophostin (Figure 1C), from *Streptomyces* have this same structural motif and have been reported as hormone sensitive lipase and acetylcholinesterase inhibitors, respectively.[18,19] These compounds are estimated to be derived from a similar pathway as the GBL biosynthetic pathway based on their structural similarity.

The most studied GBL compound is A-factor (Figure 1B) from *Streptomyces griseus*.[20,21] The GBL structure is formed from the condensation of beta-ketoacyl acyl carrier protein (ACP) and dihydroxyacetone phosphate by the A-factor synthase AfsA followed by successive reduction by BprA and dephosphorylation.[22] AfsA homologues are common in streptomycetes where they have been shown to be involved not just in GBL biosynthesis but also in the production of gamma-butenolides and furans.[6,23–26]

Recently, we showed that the AfsA homologue Spt9 in *Salinispora* bacteria is responsible for the construction of the salinipostins and its volatile byproducts, salinilactones.[2,27,28] The *spt9* gene is the terminal gene of a nine-gene biosynthetic locus (Figure 1A) that is broadly conserved in *Salinispora* species[29] (*spt* was annotated as *butyrolactone 1* in this reference). Herein, we report the functional characterization of *spt* genes, *spt6* and *spt9*, toward salinipostin biosynthesis and show that the *spt* gene cluster is also responsible for the synthesis of novel, natural GBLs as coproducts of salinipostin biosynthesis. Furthermore, we revealed that *spt*-like biosynthetic gene clusters are broadly distributed among actinomycete genera, suggesting its important role in bacterial signaling.

RESULTS AND DISCUSSION

Discovery of Gamma-Butyrolactone Compounds from *Salinispora* Species.

We previously reported the global transcriptional activity of biosynthesis gene clusters in *Salinispora* species and showed that the *spt* locus was involved with salinipostin biosynthesis through genetic inactivation of *spt9* and a concomitant loss of salinipostin.[2] Upon reexamination of the *S. tropica* CNB-440 *spt9*-deletion mutant in comparison with the native CNB-440 strain by liquid chromatography–mass spectrometry (LC-MS), we identified compounds in addition to the salinipostins that were also abolished in the mutant (Figure 2B). Inspection of the molecular formulas of compounds 2 ($C_{11}H_{19}O_4$, *m*/*z* 215.1280, $[M + H]^+$ calcd. 215.1278) and 3 ($C_{10}H_{17}O_4$, *m*/*z* 201.1126, $[M + H]^+$ calcd. 201.1121) suggested that they could be simple, A-factor-like GBL compounds (Figure S1).

Generally, the production levels of GBLs in native strains are quite modest, reflecting the low effective concentration of the signaling molecules (e.g., A-factor, 10^{-9} M).[30] As such,

significant effort is often required to isolate and characterize GBLs as in the case of SCB-1 and IM-2 in which several hundred liters of cultures were analyzed.[31,32] To enhance the poor productivity of the *S. tropica* GBL compounds, we grew strain CNB-440 with Amberlite XAD-7HP resin to achieve an approximately 50-fold enhancement of GBL production (Figure S2). With this method, we purified 1.2 mg of the most abundant GBL (Sal-GBL1, 2) from 3 L culture for comprehensive NMR analysis (Figures S3–S6). On the basis of the 1D and 2D NMR analysis, the structure of 2 was confirmed as a new natural GBL containing an iso-hexanoyl side chain (Figure 2A). The circular dichroism spectrum of 2 exhibited similar Cotton effects as the natural form of synthetic 3-(*R*)-A-factor[33,34] (Figure S7), therefore establishing the stereochemistry at C-3 in 2 as *R*. This stereochemical configuration is consistent with the stereochemistry at the same carbon in salinipostin (C-2).[16,35] A second analogue (SalGBL2, 3) was elucidated with a pentanoyl side chain (Figure 2A, 3) based on the LC-MS comparison with a chemically synthesized standard (Figures S8–S11).

We observed that compounds 2 and 3 are also produced in the other species of *Salinispora* producing salinipostins, namely, *S. arenicola* CNS-205, *S. mooreana* CNT-150 and *Salinispora* sp. RL08-036-SPS-B (Figures 2B and S10), representing the first identification of A-factor-like GBL compounds in the genus of *Salinispora*. The production of 2, 3, and salinipostins was also completely abolished in *S. arenicola* CNS-205 Δ*spt9* and *Salinispora* sp. RL08-036-SPS-B Δ*spt9*, reinforcing that *spt9* is essential for their biosynthesis (Figures 2B and S10).

On the basis of the distinct chemical features of the salinipostins and Sal-GBLs and the gene composition of the *spt* gene cluster, we suspected that the biosynthetic pathway likely diverges at an early common intermediate. As such, we knocked out the putative nucleotide diphosphate-kinase *spt6* gene in *Salinispora* sp. RL08-036-SPS-B and showed that this mutant produced 2, which lacks a phosphotriester, but not salinipostins, with the phosphotriester group (Figure 2B). These results are consistent with our proposed, diverging pathway (Figure 3), whereby subsequent pyrophosphate formation via *Spt*6 redirects the biosynthetic pathway to salinipostins.

In vitro Reconstitution of the Gamma-Butyrolactone Structure.

To further evaluate salinipostin biosynthesis and its branchpoint with GBL synthesis, we next evaluated the *in vitro* activity of recombinant Spt9 based on prior examination of the homologous A-factor synthase AfsA.[22] We prepared the N-terminus maltose-binding protein (MBP) and histidine tagged Spt9 (Spt9-H-MBP) from *E. coli* harboring pET28a-MBP-*spt9* and removed both affinity tags using TEV protease (Figure S17). We next synthesized both substrates: the beta-keto heptanoyl *N*-acetylcysteamine thioester (SNAC) (4) as a substrate mimic of the ACP-bound substrate and dihydroxyacetone phosphate (5).[36] We first observed the consumption of 4 in the enzymatic reaction mixture; however, a product peak was not detected in the LC-MS analysis. Therefore, we analyzed the reaction mixture using LC-MS immediately after short incubation periods. Incubation of tag-free Spt9 with substrates 4 and 5 (1 mM, each) in a phosphate-citrate buffer at 30 °C for 10 min yielded a plausible phosphorylated butenolide compound (7) having the anticipated molecular formula

$C_{10}H_{17}O_7P$ (*m*/*z* 277.0481, $[M–H]^-$ calcd. 277.0483) and phosphate fragment ion at *m*/*z* 96.9709 ($[M–H]^-$ calcd. for H_2O_4P, 96.9696; Figure 4B and S18).

In A-factor biosynthesis, butenolide formation is followed by reduction with BprA, which is encoded immediately downstream of afsA.[22] The *spt* gene cluster, however, does not encode a bprA homologue nor elsewhere nearby. Thus, we chose to incubate enzymatically produced 7 with the lysate prepared from the *S. tropica* CNB-440 Δ*spt9* deletion mutant along with NADPH (Figure 4B). In this way, we produced compound 8 (*m*/*z* 279.0632, ($[M–H]^-$ calcd. 279.0639), which we validated by LC-MS analysis with synthetically prepared Sal-GBL2 phosphate (8). Chemical reduction of the C–C double bond in 7 with $NaBH_3CN$ also gave a relatively stable compound that eluted at the same retention time as the synthetic GBL-phosphate (8). These results are consistent with previous reports where the expression of recombinant AfsA in *E. coli* resulted in the production of A-factor-like compounds in the host, and reduction of butenolide was suggested to be catalyzed by the endogenous reductase in the bacteria.[8,22] Thus, despite their low sequence homology at 35.8% (pairwise positive, ClustalW alignment), our data unequivocally confirm that Spt9, like AfsA, catalyzes butenolide formation.

Although we assumed that passive cellular uptake of GBL-phosphate is unlikely based upon its polarity and negative charge, supplementation of *S. tropica* CNB-440 Δ*spt9* with synthetic 8 recovered the production of salinipostin B, which contains an *n*-butyl side chain (Figures 4C and S19). Conversely, the supplementation of GBLs 2 and 3 did not recover salinipostin production. Only in the case of supplementation with 8 were other possible salinipostin analogues containing the C_4H_8 side chain also detected (Figures S20–S22), while natural salinipostins containing different side chains were not generated (Figure 4C, ii,v). These results support our hypothesis that salinipostin biosynthesis is initiated with the construction of the GBL. Furthermore, compound 3 was detected in the extract of *S. tropica* CNB-440 Δ*spt9* supplemented with synthetic 8 (Figure S23). Consistent with that observation, lysate of *S. tropica* CNB-440 Δ*spt9* similarly showed weak dephosphorylation activity (Figure S24). The incubation of 8 with commercial alkaline phosphatase (CIP) reliably gave 3 (Figure S25). Because there are no dedicated phosphatases in the *spt* gene cluster, we assume that this dephosphorylation was catalyzed by a nonspecific bacterial phosphatase, as similarly implied in A-factor biosynthesis.

Our investigations of salinipostin biosynthesis indicated that the GBL-phosphate 8 is a biosynthetic intermediate of salinipostin. As a prelude to phosphodiester ring formation, we hypothesized that activation of the phosphate group of 8 is an absolute requirement. Biochemically, this is achieved through pyrophosphate formation as seen in the formation of the phosphodiester ring in cyclic-AMP, where adenylate cyclase converts ATP into cyclic AMP along with releasing a pyrophosphate as a leaving group.[37] Our mutant analysis confirmed that the *spt*6 gene encoding a diphosphate kinase is essential for the production of salinipostin as described above. Therefore, we further investigated the *in vitro* function of Spt6. We tested the enzymatic phosphorylation using the His-tagged Spt6 (H-Spt6) purified from *E. coli* harboring pET28a-*spt*6 (Figure S26). Incubation of H-Spt6 and 8 with ATP and Mg^{2+} in HEPES buffer (pH 8) yielded the GBL-pyrophosphate (9), showing a fragment ion at *m*/*z* 176.9358 ($[M–H]^-$ calcd. for $H_3O_7P_2$, 176.9359) derived from the pyrophosphate

group in both hydrophilic interaction chromatography (HILIC) LC-MS/MS (Figure 4D,E) and reversed-phase (RP) LC-MS/MS analyses (Figure S27). Thus, we hypothesize that 9 is the first dedicated biosynthetic intermediate in the salinipostin pathway and is required for the formation of the cyclic phosphodiester group. Few enzymes catalyze phosphorylation reactions on phosphorylated substrates in secondary metabolism. One example is CalQ, which forms a diphosphate secondary metabolite, the protoxin phosphocalyculin A from toxic calyculin A,[38] but Spt6 shares low sequence identity with CalQ (13.9%, ClustalW alignment).

We anticipate that the remainder of the pathway from the GBL pyrophosphate 9 to the salinipostins and its highly unusual phosphotriester core involves additional enzymes encoded within the *spt* locus (Figure 3). Biochemical experiments are presently underway.

Distribution and Gene Content of Salinipostin-Like Biosynthetic Gene Clusters.

The salinipostin biosynthetic gene cluster (*spt1–9*) is conserved at the genus level in *Salinispora*.[29] Using a targeted genome-mining approach, we identified nine genera in addition to *Salinispora* that maintain *spt*-like biosynthetic gene clusters (representative biosynthetic gene clusters are shown in Figure 5). The *spt*-like gene clusters were identified in six diverse Actinobacterial families: *Nocardiaceae, Tsukamurellaceae, Mycobacteriaceae, Pseudonocardiaceae, Dietziaceae,* and *Streptomycetaceae*. Notably, *spt*-like gene clusters were found outside of the *Streptomycetaceae* where the gamma-butyrolactone A-factor and *spt9* homologue afsA were characterized. *Spt1*, *spt3*, *spt5*, *spt6*, *spt7*, and *spt9* are conserved across all *spt*-like gene clusters (Figure 5), although *spt2−3* and *spt6−9* gene fusions were observed in some strains. *Spt8* was uniquely observed in the *Salinispora spt* gene cluster. The organization of the *spt* biosynthetic gene cluster is largely conserved across multiple families of bacteria, ultimately suggesting that these diverse taxa have the capability to produce salinipostin-like phophotriester GBLs. A detailed analysis of *spt* gene distribution, organization, and evolutionary history was the subject of another study.[39]

In conclusion, we established the early steps of salinipostin biosynthesis in *Salinispora* bacteria and showed that the phosphorylated GBL 8 is the branchpoint metabolic intermediate to the salinipostins and the newly identified Sal-GBL1 (2) and Sal-GBL2 (3) A-factor-like natural compounds. Intriguingly, the *spt* locus may thus have a dual biological purpose in the construction of both butyrolactone chemotypes whose native *Salinispora* functions have yet to be determined. While no small molecules from *Salinispora* have yet been experimentally established as autoregulators, *Salinispora* also produce acyl-homoserine lactones that are known to mediate quorum sensing in Gram-negative bacteria.[40] Future investigations on the function of these molecules will undoubtedly shed light on the regulatory mechanism of secondary metabolism in *Salinispora*.

Our work also opens the door to establishing the biochemical logic for the construction of salinipostin's highly unusual phosphotriester functionality that is shared by the streptomycete molecules cyclipostin and cyclophostin. The high energy GBL pyrophosphate 9 is chemically predisposed for an intramolecular cyclization reaction with a loss of phosphate to a cyclic phosphodiester GBL intermediate (Figure 3). Condensation with a fatty alcohol constructed with Spt2/4/5 theoretically completes the pathway to the

salinipostins. This proposed pathway anticipates the biosynthesis of cyclipostin and cyclophostin, which together with the salinipostins, may be more common in actinomycete biology than previously thought given the wide distribution of *spt*-like biosynthesis gene clusters (Figure 5). As such, we hypothesize that salinipostin-like phosphotriester GBLs may function as a new class of signaling molecules. Interrogation of salinipostin biosynthetic gene clusters may represent a key step in further unlocking the biosynthetic potential in *Salinispora* and other actinomycetes.

METHODS

Gene Deletion of *spt9*.

i. *Salinispora tropica* CNB-440/Δ*spt9* was generated previously.[2]

ii. *Salinispora arenicola* CNS-205/Δ*spt9*.

The DNA fragment A containing the upstream 3.0 kb region of *spt9* was amplified by PCR with primers 1, 5′-ccccgggctgcaggaattcacctcgaacgcgcctactggcac-3′ (annealing sequence boldfaced), and 2, 5′-caccatcgatggttatagccgggtgtcggtcatcggttg-3′, and fragment B containing the downstream 3.0 kb region of *spt9* was amplified by PCR with primers 3, 5′-accgacacccggctataaccatcgatggtgatctgtcgg-3′, and 4, 5′-ccagcctacacatcgaattcgcctgcgcaacgcatagtggagatc-3′. Fragments A and B were assembled with the pIJ773-derived fragment amplified by primers 5, 5′-gaattcctgcagcccgggggatc-3′, and 6, 5′-gaattcgatgtgtaggctggag-3′ using the Gibson assembly technique (kit was purchased from New England Biolabs), to yield pIJ773-Δ*spt9*. The gene deletion vector pIJ773-Δ*spt9* was introduced into *S. arenicola* CNS-205 via intergeneric conjugation. The Apr^R exoconjugates from double-crossover were selected as the previously reported procedure.[41] *S. arenicola* CNS-205/Δ*spt9* was isolated from Apr^S clones selected from the repeated subculture of Apr^R clones on the aparamycin-free agar plate.[27]

iii. *Salinispora* sp. RL08-036-SPS-B/Δ*spt9* and *Salinispora* sp. RL08-036-SPS-B/Δ*spt*6.

The gene inactivation experiments of *spt9* and *spt*6 in *Salinispora* sp. RL08-036-SPS-B were performed using a PCR-targeting method. The coding region of *spt9* was first replaced with an apramycin resistant gene *aac(3)IV* in cosmid 12E4-bla, which was isolated from the genomic library of *Salinispora* sp. RL08-036-SPS-B. The *aac(3)IV* disruption cassette was amplified from pHY773 by PCR primers with homology extensions targeting *spt9* (primer pair, 5′- atgaccgacacccggctactgaccccacctcacacgaccattccggggatccgtcgacc-3′ and 5′-ctgagcctctcgtcgagcaccccggtcaacacctggcgttgtaggctggagctgcttc-3′). The resulting vector 12E4-bla (Δ*spt9*) was passaged through *E. coli* S17–1 and then introduced into *Salinispora* sp. RL08-036-SPS-B via intergeneric conjugation. The apramycin^R exconjugants were screened by PCR for the double crossover mutants. Inactivation of *spt*6 was conducted similarly, except that an *aac(3)IV-ermE**p disruption cassette (primer pair, 5′-cctgacccacgatccggacaagcagcgctatcacggcactcagttcccgccagcctgct-3′ and 5′-

gaaagcgataccgcgtggctgcccaccacgatgaaatcctaccaaccggcacgattgtg-3′) was used to prevent the potential polar effects on downstream genes.

LC-MS Analysis of Salinipostins and Sal-GBLs.

Each strain was cultured in a 250 mL Erlenmeyer flask containing 50 mL of medium A1+BFe (A1 plus 1 g L^{-1} $CaCO_3$, 40 mg L^{-1} $Fe_2(SO_4)_3{\cdot}4H_2O$, 100 mg L^{-1} KBr) at 28 °C with shaking at 230 rpm (New Brunswick Innova 2300). Sterile Amberlite XAD-7HP resin (1 g, Sigma-Aldrich) was added to each flask after 48 h, and the fermentation was continued for an additional 4 days. The resins and cells were collected by filtration using cheese cloth or centrifugation, washed with distilled water, and soaked in acetone for 2 h. The extract was concentrated *in vacuo* and the resultant residue dissolved in methanol. After filtration, an aliquot of the extract was subjected to LC-MS. For the salinipostin analysis, HR-LC-MS analysis was performed using a Phenomenex Kinetex XB-C_{18} column (2.6 μm, 100 × 4.6 mm, 100 Å) with the following conditions: positive mode; mobile phase A: 0.1% formic acid in H_2O (v/v); mobile phase B: 0.1% formic acid in MeCN (v/v); 1.0 mL/min, 0–8 min (80–90% B), 8–13 min (90%–100% B), 13–15 min (100% B). The ion at *m*/*z* 445.2714 (salinipostin G and analogues), 459.2870 (salinipostin B and analogues), and 473.3027 (salinipostin analogues) corresponding to the $[M + H]^+$ ion was analyzed in the extracted ion chromatograms (EIC). Low-resolution LC-MS analysis was performed using a Phenomenex Kinetex XB-C_{18} column (2.6 μm, 100 × 4.6 mm, 100 Å) with the following conditions: positive mode; mobile phase A: 0.1% formic acid in H_2O (v/v); mobile phase B: 0.1% formic acid in MeCN (v/v); 1.0 mL/min, 0–8 min (80–90% B), 8–10 min (90%–100% B), 10–15 min (100% B), with a flow splitter. For the Sal-GBLs, HR-LC-MS analysis was performed using a Phenomenex Luna C_{18}(2) column (5.0 μm, 150 × 4.6 mm, 100 Å) with the following conditions: positive mode and negative mode; mobile phase A: 0.1% formic acid in H_2O (v/v); mobile phase B: 0.1% formic acid in MeCN (v/v); 0.7 mL/min, 0–1 min (20% B), 1–21 min (20%–100% B), and 21–31 min (100% B). Ions at *m*/*z* 215.1278 and 201.1121 (Sal-GBL1 (2) and Sal-GBL2 (3), respectively) corresponding to the $[M + H]^+$ ion were analyzed in the EIC in positive mode. The ion at *m*/*z* 199.0976 (Sal-GBL2 (3)) corresponding to the $[M–H]^-$ ion was analyzed in the EIC in negative mode.

Enzymatic Reaction of Spt9.

The purified *Spt9*-H-MBP and tag-free Spt9 were used for the enzymatic reaction. The reaction mixture containing 100 μM of Spt9-H-MBP, 1 mM beta-keto heptanoyl N-acetylcysteamine thioester (beta-keto heptanoyl SNAC; 4), and 1 mM of dihydroxyacetone phosphate (DHAP, 5) was incubated in 50 mM McIlvaine buffer (pH 7.0) at 30 °C for 10 min. One volume of MeCN was added to the reaction mixture and then centrifuged at 15 000*g* for 2 min. The filtered supernatant was analyzed by LC-MS using a Phenomenex Luna C_{18}(2) column (5.0 μm, 100 × 4.6 mm, 100 Å) with the following conditions: negative mode; mobile phase A: 0.1% formic acid in H_2O (v/v); mobile phase B: 0.1% formic acid in MeCN (v/v); 0.7 mL/min, 0–3 min (10% B), 3–14 min (10%–100% B), and 14–18 min (100% B). The ions at *m*/*z* 277.0483 (compound 7) and 279.0639 (compound 8) corresponding to the $[M–H]^-$ ion were analyzed in the extracted ion chromatograms (EIC). The collision energy in the MS/MS analysis of 7 was 10 eV.

Reduction of Butanolide Using $NaBH_3CN$.

Fifty microliters of freshly prepared $NaBH_3CN$ solution (10 mM in EtOH) was added to the Spt9 enzymatic reaction mixture and incubated at RT for 30 min. To this solution, four volumes of 25 mM ammonium acetate buffer (pH 7.6) was added and then applied to the weak anion exchange resin, Macro-prep DEAE (Bio-Rad), packed in a glass pipet (column volume: 0.5 mL). The column was washed with buffer (25 mM ammonium acetate buffer, 20% MeOH in H_2O (v/v), pH 7.6) and eluted with 1% NH_4OH and 20% MeOH aqueous solution (v/v/v). The eluent was filtered and subjected to the LC-MS analysis under the same conditions as the *Spt9*-reaction analysis.

Reduction of Butenolide Using *S. tropica* Lysate.

Lysate was prepared from 25 mL of *S. tropica* CNB-440/Δ*spt9* culture. The mutant was cultured for 4–6 days in A1 media without resin. Cells were harvested from the culture by centrifugation (5000*g*) and washed with buffer (10 mM Tris-HCl, 330 mM NaCl, 10% (v/v) glycerol, 0.5 mM dithiothreitol (DTT), pH 7.5). Next, the cells were suspended in buffer and sonicated on ice. After the removal of cell debris by centrifugation (15 000*g*, 4 °C, 10 min), the supernatant was concentrated by ultrafiltration using a Centriprep centrifugal filter YM-10 (Merck Millipore). The resultant solution (protein 15 mg mL^{-1}, determined by Bradford assay) was used for the butanolide reduction reaction. This lysate was added to the Spt9 reaction mixture with NADPH (final concentration 1 mM) and then incubated at 30 °C for 1 h. The reaction was stopped by the addition of one volume of MeCN and then centrifuged at 15 000*g* for 2 min. The supernatant was applied to the LC-MS analysis under the same condition as the Spt9-reaction analysis.

Enzymatic Reaction of Spt6.

A 50 μL reaction contained 20 μM ***Spt***6, 1 mM compound 8, 1 mM ATP, 20 mM $MgCl_2$, and 50 mM HEPES (pH 8.0). After incubation at 30 °C for 60 min, one volume of MeCN was added to the reaction mixture and centrifuged at 15 000*g* for 5 min. The supernatant was analyzed by LC-MS/MS under two conditions: (1, Figure 4D,E) TSKgel Amide-80 HR (5 μm, 4.6 × 250 mm, Tosoh); negative mode; mobile phase A: 10 mM ammonium formate H_2O; mobile phase B: 10 mM ammonium formate in MeCN/H_2O (9:1, v/v); 0–3 min (90% B, 0.7–0.5 mL/min), 3–25 min (90–50% B, 0.5 mL/min), and 25–30 min (50% B, 0.5 mL/min) and (2, Figure S27) Phenomenex Luna C_{18}(2) column (5.0 μm, 100 × 4.6 mm, 100 Å); negative mode; mobile phase A: 0.1% formic acid in H_2O (v/v); mobile phase B: 0.1% formic acid in MeCN (v/v); 0.7 mL/min, 0–3 min (10% B), 3–14 min (10–100% B), and 14–18 min (100% B). Ions at *m*/*z* 279.0639 (compound 8) and 359.0302 (compound 9) corresponding to the $[M–H]^-$ ion were analyzed in the extracted ion chromatograms (EIC). The collision energy in the MS/MS analysis of 9 was 10 eV.

Feeding Experiments.

To a 50 mL preliminary culture of *S. tropica* CNB-440/Δ*spt9*, isolated Sal-GBL1 (2, 300 μg) and synthesized racemic Sal-GBL2 (3, 300 μg) in MeOH or synthesized racemic compound 8 (300 μg) in MeOH were independently added and cultured at 28 °C for 1 day with shaking. Autoclaved Amberlite XAD-7HP was added to each culture and fermented for an

additional 3 days. The cells and resins were harvested by centrifugation, washed with water, and then extracted with acetone for 2 h. The extract was filtered and concentrated *in vacuo* using rotary evaporation. After suspension in MeOH, the aliquot was applied to LC-MS for salinipostin and Sal-GBLs analysis as described above.

Structure Elucidation of Sal-GBL1 (2).

Structure elucidation of Sal-GBL1 (2) was accomplished through NMR and CD experiments. The purified compound was dissolved in 0.5 mL of $CDCl_3$. ^1H NMR, a gradient COSY, a gradient HSQC, and a gradient HMBC ($^3J_{CH}$ = 8 Hz) were measured in a 5 mm NMR tube. The residual $CHCl_3$ signal at 7.26 ppm in the ^1H NMR spectrum and the $^{13}CDCl_3$ signal at 77.16 ppm in the ^{13}C NMR spectra were used as internal references. All the proton and carbon signals were assigned based on the 2D NMR experiments (Figures S3–S6, Table S1). Keto–enol tautomerization gave small signal sets in the ^1H NMR spectrum. The CD spectrum of 2 was measured in MeOH (Figure S7): 279 nm ($\Delta\varepsilon$ + 0.465), 229 nm ($\Delta\varepsilon$ + 0.342). The observed Cotton effect was compared with that of synthetic 3-(*R*)-A-factor in the literature reported by Mori:[33,34] 283.5 nm ($\Delta\varepsilon$ + 0.699), 221.0 nm ($\Delta\varepsilon$ + 0.420).

Distribution and Gene Content of Salinipostin-Like Biosynthetic Gene Clusters.

ClusterScout searches were performed to identify salinipostin-like biosynthetic gene clusters in other genomes[42] using the following Pfam functions: *spt1*, Pfam00391 and Pfam01326; *spt2*, Pfam00501; *spt4*, Pfam00550; *spt5*, Pfam07993; *spt6*, Pfam00334; *spt7*, Pfam01040; *spt8*, Pfam00296; *spt9*, Pfam03756. Independent searches were run with a minimum requirement of either three, four, or five Pfam matches, a maximum distance of <10 000 bp between each Pfam match, and a minimum distance of 1 bp from the scaffold edge. The boundaries of each match were extended by a maximum of 10 000 bp to help return full biosynthetic operons. For some searches, the *spt9*/*afsA* Pfam was defined as essential. MultiGeneBlast[43] was also used to query the contiguous salinipostin *spt1*−*9* gene cluster from *S. tropica* CNB-440 against the NCBI GenBank Bacteria BCT subdivision database. Biosynthetic clusters retrieved from each ClusterScout and MultiGeneBlast search were inspected for each of the nine *spt* Pfam hooks, and biosynthetic gene clusters with similar organization to *spt* in *S. tropica* CNB-440 were saved for further analyses.

Supplementary Material

Refer to Web version on PubMed Central for supplementary material.

ACKNOWLEDGMENTS

We thank B. M. Duggan from UC San Diego for assistance with NMR measurements. We are grateful to M. R. Ghadiri and L. J. Leman at the Scripps Research Institute for their help in the collection of CD measurements. We also thank our UC San Diego colleagues Z. D. Miles, G. C. A. Amos, H. Machado, M. C. Kim, X. Tang, H. Luhavaya, J. Li, S. M. K. McKinnie, and J. R. Chekan for experimental advice.

Funding

This work was supported by National Institutes of Health grant GM085770 (to B.S.M. and P.R.J.), the Japan Society for Promotion of Science (to Y.K., JSPS Overseas Research Fellowship), the Uehara Memorial Foundation

(to T.A., Research Fellowship), and the National Science Foundation Graduate Research Fellowship Program under Grant No. DGE-1650112 (to K.E.C).

REFERENCES

(1). Nett M, Ikeda H, and Moore BS (2009) Genomic basis for natural product biosynthetic diversity in the actinomycetes. Nat. Prod. Rep 26, 1362–1384. [PubMed: 19844637]

(2). Amos GCA, Awakawa T, Tuttle RN, Letzel A-C, Kim MC, Kudo Y, Fenical W, S. Moore B, and Jensen PR (2017) Comparative transcriptomics as a guide to natural product discovery and biosynthetic gene cluster functionality. Proc. Natl. Acad. Sci. U. S. A 114, E11121–E11130.

(3). Aroonsri A, Kitani S, Hashimoto J, Kosone I, Izumikawa M, Komatsu M, Fujita N, Takahashi Y, Shin-ya K, Ikeda H, and Nihira T. (2012) Pleiotropic control of secondary metabolism and morphological development by KsbC, a butyrolactone autoregulator receptor homologue in Kitasatospora setae. Appl. Environ. Microbiol 78, 8015–8024. [PubMed: 22961899]

(4). Li X, Wang J, Li S, Ji J, Wang W, and Yang K. (2015) ScbR-and ScbR2-mediated signal transduction networks coordinate complex physiological responses in Streptomyces coelicolor. Sci. Rep 5, 14831. [PubMed: 26442964]

(5). Suroto DA, Kitani S, Miyamoto KT, Sakihama Y, Arai M, Ikeda H, and Nihira T. (2017) Activation of cryptic phthoxazolin A production in Streptomyces avermitilis by the disruption of autoregulator-receptor homologue AvaR3. J. Biosci. Bioeng 124, 611–617. [PubMed: 28728974]

(6). Takano E. (2006) γ-Butyrolactones: Streptomyces signalling molecules regulating antibiotic production and differentiation. Curr. Opin. Microbiol 9, 287–294. [PubMed: 16675291]

(7). Hsiao NH, Nakayama S, Merlo ME, de Vries M, Bunet R, Kitani S, Nihira T, and Takano E. (2009) Analysis of two additional signaling molecules in Streptomyces coelicolor and the development of a butyrolactone-specific reporter system. Chem. Biol 16, 951–960. [PubMed: 19778723]

(8). Ando N, Matsumori N, Sakuda S, Beppu T, and Horinouchi S. (1997) Involvement of afsA in A-factor biosynthesis as a key enzyme. J. Antibiot 50, 847–852.

(9). Horinouchi S, and Beppu T (1992) Autoregulatory factors and communication in actinomycetes. Annu. Rev. Microbiol 46, 377–398. [PubMed: 1444261]

(10). Horinouchi S. (2002) A microbial hormone, A-factor, as a master switch for morphological differentiation and secondary metabolism in Streptomyces griseus. Front. Biosci., Landmark Ed 7, 2045–2057.

(11). Udwary DW, Zeigler L, Asolkar RN, Singan V, Lapidus A, Fenical W, Jensen PR, and Moore BS (2007) Genome sequencing reveals complex secondary metabolome in the marine actinomycete Salinispora tropica. Proc. Natl. Acad. Sci. U. S. A 104, 10376–10381. [PubMed: 17563368]

(12). Duncan KR, Crüsemann M, Lechner A, Sarkar A, Li J, Ziemert N, Wang M, Bandeira N, Moore BS, Dorrestein PC, and Jensen PR (2015) Molecular networking and pattern-based genome mining improves discovery of biosynthetic gene clusters and their products from Salinispora species. Chem. Biol 22, 460–471. [PubMed: 25865308]

(13). Jensen PR, Williams PG, Oh DC, Zeigler L, and Fenical W. (2007) Species-specific secondary metabolite production in marine actinomycetes of the genus Salinispora. Appl. Environ. Microbiol 73, 1146–1152. [PubMed: 17158611]

(14). Jensen PR, Moore BS, and Fenical W. (2015) The marine actinomycete genus Salinispora: A model organism for secondary metabolite discovery. Nat. Prod. Rep 32, 738–751. [PubMed: 25730728]

(15). Ziemert N, Lechner A, Wietz M, Millan-Aguinaga N, Chavarria KL, and Jensen PR (2014) Diversity and evolution of secondary metabolism in the marine actinomycete genus Salinispora. Proc. Natl. Acad. Sci. U. S. A 111, E1130–E1139. [PubMed: 24616526]

(16). Schulze CJ, Navarro G, Ebert D, Derisi J, and Linington RG (2015) Salinipostins A-K, long-chain bicyclic phosphotriesters as a potent and selective antimalarial chemotype. J. Org. Chem 80, 1312–1320. [PubMed: 25584395]

(17). Yoo E, Schulze CJ, Stokes BH, Onguka O, Yeo T, Mok S, Gnädig NF, Zhou Y, Kurita K, Foe IT, Terrell SM, Boucher MJ, Cieplak P, Kumpornsin K, Lee MCS, Linington RG, Long JZ,

Uhlemann AC, Weerapana E, Fidock DA, and Bogyo M. (2020) The antimalarial natural product salinipostin A identifies essential α/β serine hydrolases involved in lipid metabolism in P. falciparum parasites. Cell Chem. Biol 27, 143–157. [PubMed: 31978322]

(18). Vertesy L, Beck B, Bronstrup M, Ehrlich K, Kurz M, Muller G, Schummer D, and Seibert G. (2002) Cyclipostins, novel hormone-sensitive lipase inhibitors from Streptomyces sp. DSM 13381. II. Isolation, structure elucidation and biological properties. J. Antibiot 55, 480–494.

(19). Kurokawa T, Suzuki K, Hayaoka T, Nakagawa T, Izawa T, Kobayashi M, and Harada N. (1993) Cyclophostin, acetylcholinesterase inhibitor from Streptomyces lavendulae. J. Antibiot 46, 1315–1318.

(20). Horinouchi S, and Beppu T. (1994) A-factor as a microbial hormone that controls cellular differentiation and secondary metabolism in Streptomyces griseus. Mol. Microbiol 12, 859–864. [PubMed: 7934895]

(21). Horinouchi S. (2007) Mining and polishing of the treasure trove in the bacterial genus Streptomyces. Biosci., Biotechnol., Biochem 71, 283–299. [PubMed: 17284841]

(22). Kato J, Funa N, Watanabe H, Ohnishi Y, and Horinouchi S. (2007) Biosynthesis of γ-butyrolactone autoregulators that switch on secondary metabolism and morphological development in Streptomyces. Proc. Natl. Acad. Sci. U. S. A 104, 2378–2383. [PubMed: 17277085]

(23). Hsiao NH, Söding J, Linke D, Lange C, Hertweck C, Wohlleben W, and Takano E. (2007) ScbA from Streptomyces coelicolor A3(2) has homology to fatty acid synthases and is able to synthesize γ-butyrolactones. Microbiology 153, 1394–1404. [PubMed: 17464053]

(24). Corre C, Song L, O'Rourke S, Chater KF, and Challis GL (2008) 2-Alkyl-4-hydroxymethylfuran-3-carboxylic acids, antibiotic production inducers discovered by Streptomyces coelicolor genome mining. Proc. Natl. Acad. Sci. U. S. A 105, 17510–17515. [PubMed: 18988741]

(25). Arakawa K, Tsuda N, Taniguchi A, and Kinashi H. (2012) The butenolide signaling molecules SRB1 and SRB2 induce lankacidin and lankamycin production in Streptomyces rochei. ChemBioChem 13, 1447–1457. [PubMed: 22761035]

(26). Arakawa K. (2018) Manipulation of metabolic pathways controlled by signaling molecules, inducers of antibiotic production, for genome mining in Streptomyces spp. Antonie van Leeuwenhoek 111, 743–751. [PubMed: 29476430]

(27). Schlawis C, Kern S, Kudo Y, Grunenberg J, Moore BS, and Schulz S. (2018) Structural elucidation of trace components combining GC/MS, GC/IR, DFT-calculation and synthesis—Salinilactones, unprecedented bicyclic lactones from Salinispora Bacteria. Angew. Chem., Int. Ed 57, 14921–14925.

(28). Schlawis C, Harig T, Ehlers S, Guillen-Matus DG, Creamer KE, Jensen P, and Schulz S. (2020) Extending the salinilactone family. ChemBioChem 21, 1629–1632. [PubMed: 31957947]

(29). Letzel AC, Li J, Amos GCA, Millán-Aguiñaga N, Ginigini J, Abdelmohsen UR, Gaudêncio SP, Ziemert N, Moore BS, and Jensen PR (2017) Genomic insights into specialized metabolism in the marine actinomycete Salinispora. Environ. Microbiol 19, 3660–3673. [PubMed: 28752948]

(30). Hara O, and Beppu T. (1982) Induction of streptomycin-inactivating enzyme by A-factor in Streptomyces griseus. J. Antibiot 35, 1208–1215.

(31). Sato K, Nihira T, Sakuda S, Yanagimoto M, and Yamada Y. (1989) Isolation and structure of a new butyrolactone autoregulator from Streptomyces sp. FRI-5. J. Ferment. Bioeng 68, 170–173.

(32). Takano E, Nihira T, Hara Y, Jones JJ, Gershater CJ, Yamada Y, and Bibb M. (2000) Purification and structural determination of SCB1, a gamma-butyrolactone that elicits antibiotic production in Streptomyces coelicolor A3(2). J. Biol. Chem 275, 11010–11016. [PubMed: 10753903]

(33). Mori K. (1981) Synthesis and absolute configuration of A-factor, the inducer of streptomycin biosynthesis in inactive mutants of Streptomyces griseus. Tetrahedron Lett. 22, 3431–3432.

(34). Mori K. (1983) Revision of the absolute configuration of A-factor. Tetrahedron 39, 3107–3109.

(35). Okamura H, Fujioka T, Mori N, Taniguchi T, Monde K, Watanabe H, and Takikawa H. (2019) First enantioselective synthesis of salinipostin A, a marine cyclic enol-phosphotriester isolated from Salinispora sp. Tetrahedron Lett. 60, 150917.

(36). Jung SH, Jeong JH, Miller P, and Wong CH (1994) An efficient multigram-scale preparation of dihydroxyacetone phosphate. J. Org. Chem 59, 7182–7184.

(37). Tang WJ, and Gilman AG (1992) Adenylyl cyclases. Cell 70, 869–72. [PubMed: 1525824]

(38). Wakimoto T, Egami Y, Nakashima Y, Wakimoto Y, Mori T, Awakawa T, Ito T, Kenmoku H, Asakawa Y, Piel J, and Abe I. (2014) Calyculin biogenesis from a pyrophosphate protoxin produced by a sponge symbiont. Nat. Chem. Biol 10, 648–655. [PubMed: 24974231]

(39). Creamer KE, Kudo Y, Moore BS, and Jensen PR (2020) Phylogenetic analysis of the salinipostin γ-butyrolactone gene cluster uncovers new potential for bacterial signaling-molecule diversity, bioRxiv, DOI: 10.1101/2020.10.16.342204 (accessed November 1, 2020).

(40). Bose U, Ortori CA, Sarmad S, Barrett DA, Hewavitharana AK, Hodson MP, Fuerst JA, and Shaw PN (2017) Production of N-acyl homoserine lactones by the sponge-associated marine actinobacteria Salinispora arenicola and Salinispora pacifica. FEMS Microbiol. Lett 364, fnx002.

(41). Schultz AW, Oh DC, Carney JR, Williamson RT, Udwary DW, Jensen PR, Gould SJ, Fenical W, and Moore BS (2008) Biosynthesis and structures of cyclomarins and cyclomarazines, prenylated cyclic peptides of marine actinobacterial origin. J. Am. Chem. Soc 130, 4507–4516. [PubMed: 18331040]

(42). Hadjithomas M, Chen IMA, Chu K, Huang J, Ratner A, Palaniappan K, Andersen E, Markowitz V, Kyrpides NC, and Ivanova NN (2017) IMG-ABC: New features for bacterial secondary metabolism analysis and targeted biosynthetic gene cluster discovery in thousands of microbial genomes. Nucleic Acids Res. 45, D560–D565. [PubMed: 27903896]

(43). Medema MH, Takano E, and Breitling R. (2013) Detecting sequence homology at the gene cluster level with multigeneblast. Mol. Biol. Evol 30, 1218–1223. [PubMed: 23412913]

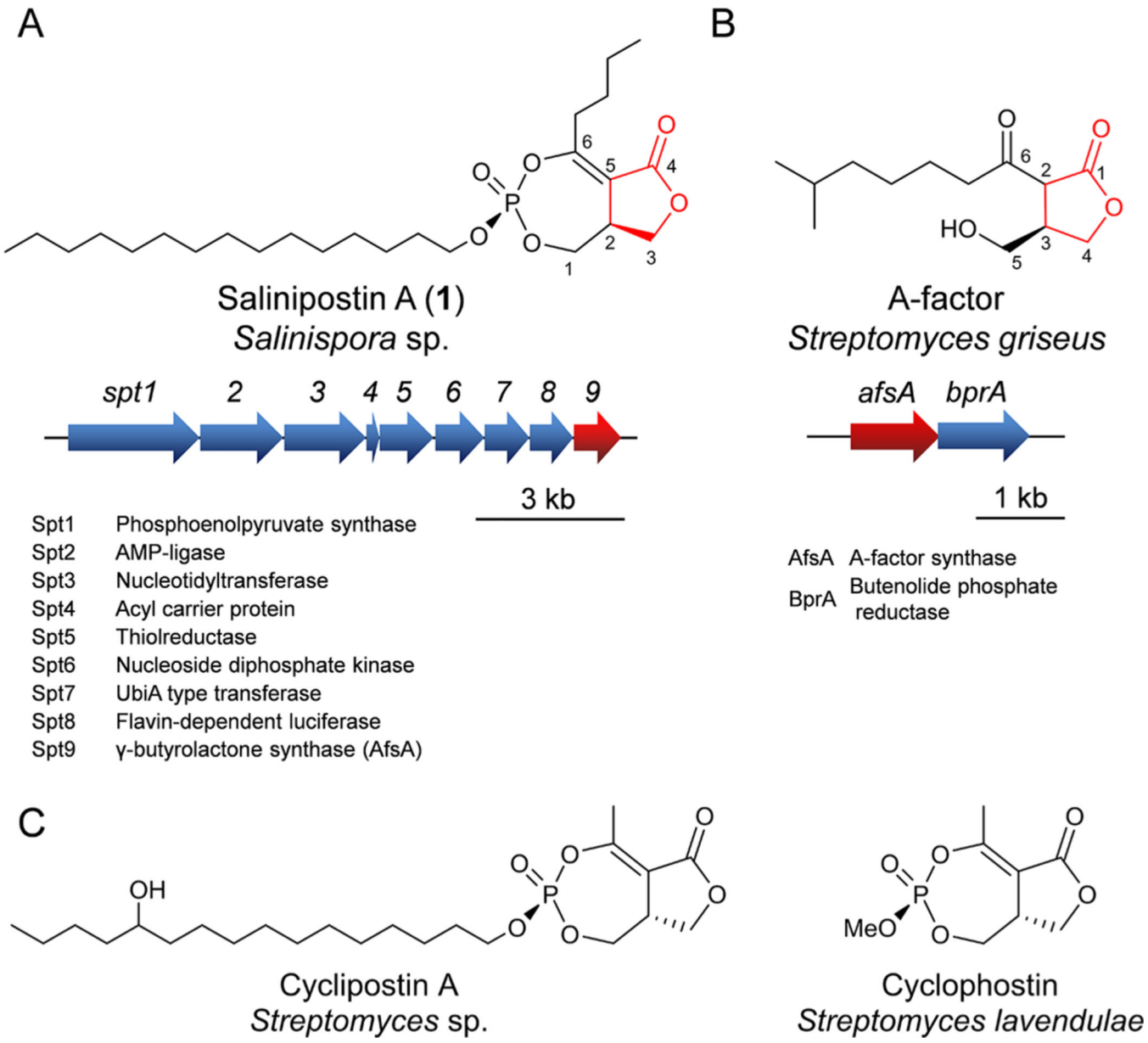

Figure 1.

Chemical structures of natural phosphotriester compounds and A-factor with their sources and biosynthetic gene clusters. (A) Salinipostin A and its biosynthesis gene cluster from *Salinispora tropica* CNB-440.[2] (B) A-factor and its biosynthesis gene cluster.[8,22] (C) Cyclipostin A and cyclophostin, whose biosynthetic genes have not yet been identified/predicted.[18,19] The gamma-butyrolactone structure and key relevant biosynthetic gene were highlighted in red in panels A and B.

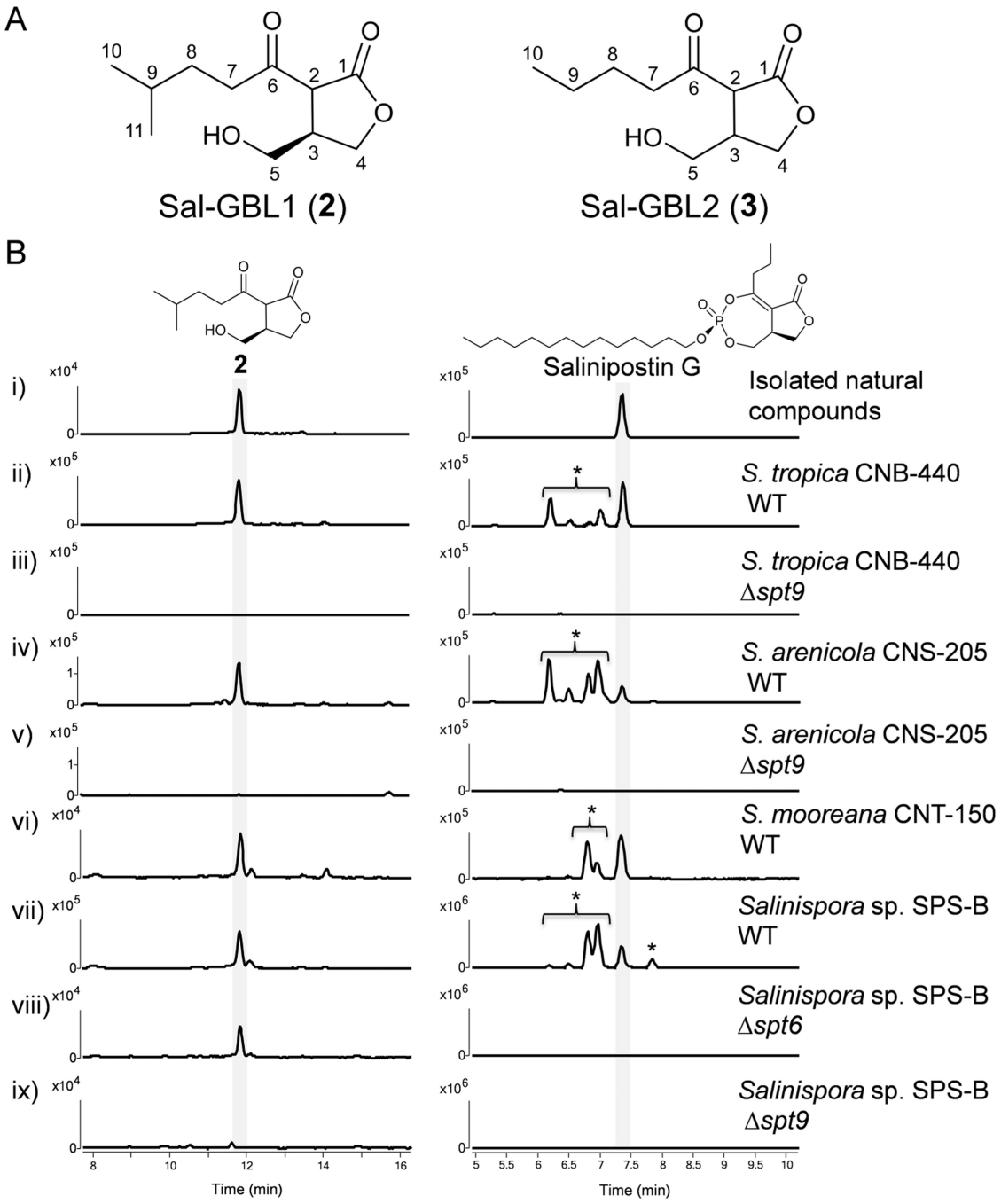

Figure 2.

Structures and mutagenesis of *spt* products. (A) Structures of new natural gamma-butyrolactones (GBLs) found in *Salinispora tropica* CNB-440, Sal-GBL1 (2) and Sal-GBL2 (3). (B) Extracted ion chromatograms (EICs) at *m*/*z* 215.1278 (Sal-GBL1, left column) and *m*/*z* 445.2714 (salinipostin G, right column) for (i) isolated natural compounds, (ii) *S. tropica* CNB-440 wild type (WT), (iii) *S. tropica* CNB-440 Δ*spt9*, (iv) *S. arenicola* CNS-205 WT, (v) *S. arenicola* CNS-205 Δ*spt9*, (vi) *S. mooreana* CNT-150, (vii) *Salinispora* sp. RL08-036-SPS-B WT, (viii) *Salinispora* sp. RL08-036-SPS-B Δ*spt*6, and (ix) *Salinispora* sp.

RL08-036-SPS-B Δ*spt9*. *Estimated as salinipostin analogues based on the high-resolution MS and/or MS/MS fragmentation pattern (Figures S12–S16).

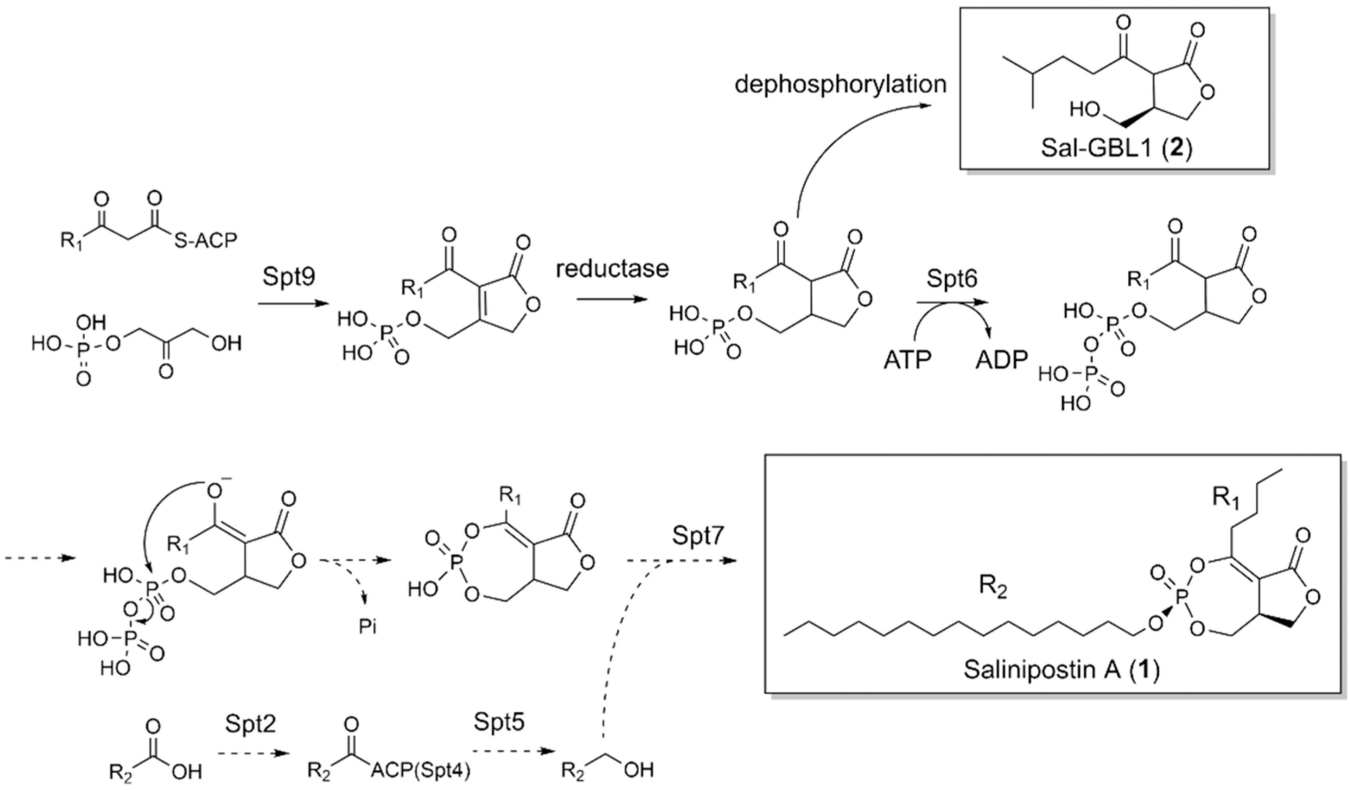

Figure 3.

Enzymatic pathway toward Sal-GBL1 (2) and Sal-GBL pyrophosphate and hypothetical biosynthetic pathway to salinipostin A (1). Solid arrows represent confirmed biochemical reactions, while dashed arrows are proposed. See Figure 1A for the putative functions of the Spt proteins.

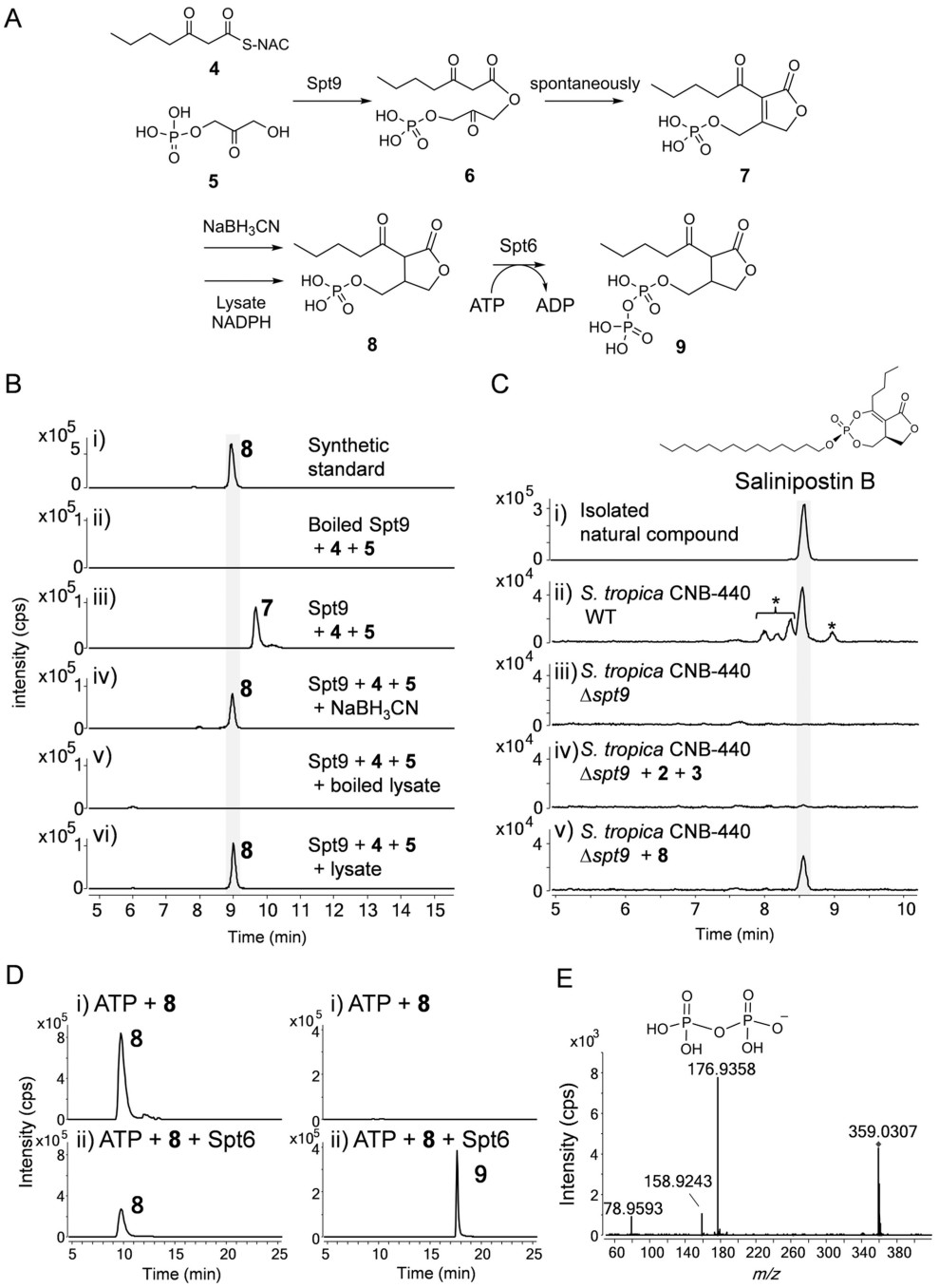

Figure 4.

Gamma-butyrolactone structure formation in the biosynthesis of salinispostin. (A) *In vitro* reaction scheme. (B) Extracted ion chromatograms (EICs) for *in vitro* reaction mixtures: (i) Synthetic standard 8, (ii) 4 and 5 treated with boiled Spt9, (iii) 4 and 5 treated with Spt9, (iv) 4 and 5 treated with Spt9, then with $NaBH_3CN$, (v) 4 and 5 treated with Spt9, then with boiled lysate, and (vi) 4 and 5 treated with Spt9, then with lysate. EIC at *m*/*z* 279.0639 for i, iv, v, and vi and *m*/*z* 277.0483 for ii and iii. (C) EICs at *m*/*z* 459.2870 for XAD extracts from the feeding experiment: (i) isolated salinipostin B, (ii) *Salinispora tropica* CNB-440

wild-type (WT), (iii) *S. tropica* CNB-440 Δ*spt9*, (iv) *S. tropica* CNB-440 Δ*spt9* supplemented with 2 and 3, and (v) *S. tropica* CNB-440 Δspt9 supplemented with 8. *Estimated as the salinipostin analogues based on the high-resolution MS and MS/MS fragmentation pattern (Figures S28 and S29). (D) HILIC-LC-MS EICs for *in vitro* reaction of phosphorylation of Sal-GBL2 phosphate (8), (i) 8, ATP and Mg^{2+} without H-Spt6 (ii) 8, ATP and Mg^{2+} with H-Spt6. EICs at *m*/*z* 279.0639 (8, left column) and *m*/*z* 359.0302 (9, right column). (E) MS/MS spectrum of 9 with the structure of fragment ion, *m*/*z* 177.

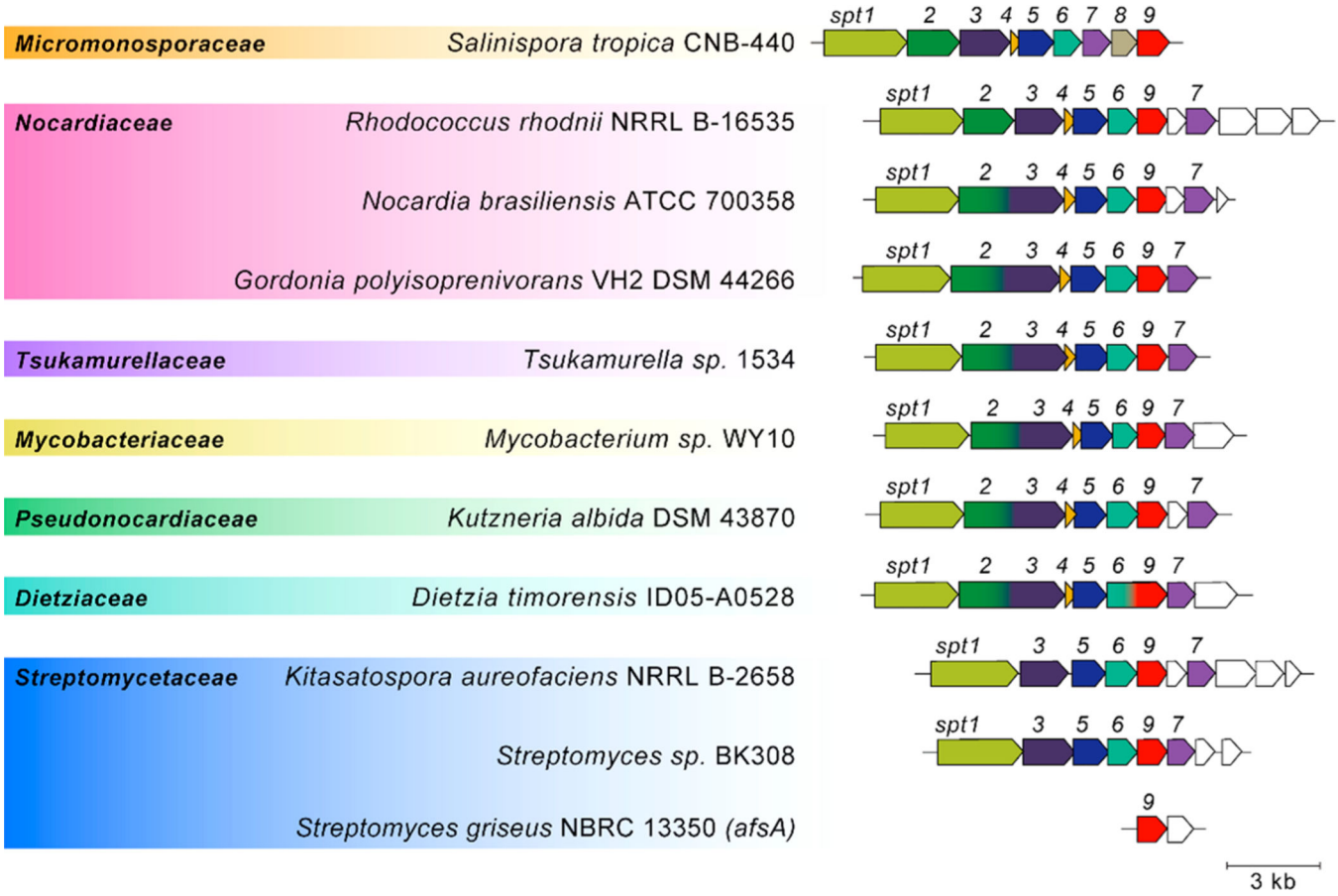

Figure 5.

Representative *spt*-like biosynthetic gene clusters observed in diverse actinomycetes. Genes are colored by the conserved Pfam function relative to *spt1−9* in *S. tropica*; white indicates no relation to *spt1−9*. *Spt*2−3 and *Spt*6−9 represent gene fusions. Products are known from *Salinispora tropica* (salinipostins and Sal-GBLs) and *Streptomyces griseus* (A-factor).